Optical Engineering 46(10), 106401 (October 2007)

# Fast new small-target detection algorithm based on a modified partial differential equation in infrared clutter

**Biyin Zhang**
**Tianxu Zhang**
**Zhiguo Cao**
**Kun Zhang**
Institute for Pattern Recognition and Artificial Intelligence
State Key Laboratory for Multispectral Information Processing Technology
Huazhong University of Science and Technology
Wuhan, 430074, China

**Abstract.** To detect and track moving dim targets against the complex cluttered background in IR image sequences is still a difficult problem because the nonstationary structured background clutter usually results in low target detectability and a high probability of false alarm. A new adaptive anisotropic filter based on a modified partial differential equation (AFMPDE) is proposed to detect a small target in such a strong cluttered background. A regularizing operator is employed to adaptively eliminate structured background and simultaneously enhance the target signal. The proposed algorithm's performance is illustrated and compared with the two-dimensional least mean square (TDLMS) adaptive filter on real IR image data. Experimental results demonstrate that the proposed novel method is fast and effective.  [DOI: 10.1117/1.2799509]

Subject terms: dim small target detection; infrared image; cluttered background; anisotropic filter; partial differential equation.

Paper 060855RR received Oct. 31, 2006; revised manuscript received Apr. 18, 2007; accepted for publication Apr. 22, 2007; published online Oct. 29, 2007.

## 1 Introduction

A crucial problem in IR search and track (IRST) surveillance systems today is the detection and recognition of weak moving targets embedded in a nonstationary cluttered background. The problem of low-contrast small-target detection and tracking arises in remote surveillance applications where the target signal amplitude is weak relative to the background clutter and noise. Nonstationary textured clutter is usually caused by atmosphere radiation, a sunlit bright cloud, or the earth's surface, so the targets are typically buried in complex clutter and have a very low signal-to-clutter ratio (SCR).[1] Traditionally, the detection and tracking of small targets in image sequences have been treated separately using the following processing steps: (1) image preprocessing, (2) target detection, and (3) multitarget tracking.

High-performance clutter suppression and target-enhancement are critical for detecting weak targets. Temporal filters,[2] spatial filters,[3] frequency domain filters,[4,5] three dimensional filters,[6,7] and matched filters[8] have been proposed. It is assumed that the appropriate application-dependent image preprocessing has already been performed. However, because of complex clutter, the preprocessing technologies cannot completely smooth edges caused by the image texture, which leads to degraded detectability and a high rate of false alarms.[1,9]

To solve this problem, the challenge is to design methods that can adaptively reduce the clutter and noise without losing significant features. Approaches that use a partial differential equation (PDE) model present a promising new option when the PDE model's significant anisotropic feature in many image processing applications is recognized. Since the PDE model was introduced by Perona and Malik,[10] much interesting research has been devoted to its theoretical and practical understanding in edge detection,[10] image segmentation,[11] image restoration,[12] and denoising and image enhancement.[13] However, it is still a new issue for the PDE model to be applied to the field of IR small-target detection.

This paper proposes a novel filter based on the PDE model to further smooth edge texture and to detect weaker targets. In Sec. 2 we introduce the Perona and Malik PDE model. In Sec. 3 we develop a novel anisotropic filter based on modified partial differential equations (AFMPDE) for background clutter suppression and target enhancement. In Sec. 4 we present the application of AFMPDE, and analyze and compare the performance of the new algorithm against the two-dimensional least mean square adaptive filter (TDLMS).[5] The paper is concluded in Sec. 5.

## 2 Perona and Malik Anisotropic Diffusion Equation

Perona and Malik proposed a nonlinear diffusion method for avoiding the blurring and localization problems of linear diffusion filtering. They applied an inhomogeneous process that reduces the diffusivity at those locations that have a larger likelihood to be edges. The diffusivity is measured by the anisotropic diffusion equation:

$$\frac{\partial u(x,y,t)}{\partial t} = \mathrm{div}\{c[|\nabla u(x,y,t)|]\,\nabla\, u(x,y,t)\}, \qquad (1)$$

where $u(x,y,t)$ is the diffused image, $t$ determines the diffusion time, and $\nabla u$ denotes the local gradient; $c(t) = \varphi'(t)/2t$ is called the weighting function, and $\varphi(t)$ is a proper function. Teboul et al. proposed several conditions on $c(t)$ for the "edge-preserving" or "edge-topping" anisotropic diffusion for the above applications.[10–13] This function is a strictly decreasing function and chosen to satisfy $c(t) \to 0$ when $t \to \infty$, which ensures high diffusion in homogeneous regions and weak diffusion near edges. As such, if the gradient is large, a discontinuity is assumed and the diffusion is stopped. Consequently, the anisotropic diffusion filter minimizes information loss by preserving object boundaries and detailed structures. Perona and Malik recommended the following weighting functions:

$$c(t) = \exp\left\{\frac{-t^2}{k^2}\right\} \quad \text{or}$$

$$c(t) = \frac{1}{1\frac{+t^2}{k^2}}. \tag{2}$$

Equation (1) can be discretized as follows using a four-nearest-neighbor discretization of the weighted Laplacian operator:

$$u_s^{l+1} = u_s^l + \lambda \sum_{p \in \eta_s} c(\nabla u_{s,p}) \nabla u_{s,p}, \tag{3}$$

where $u_s^l$ is the discretely sampled image, $s$ denotes the pixel position, and $l$ is discrete time steps iterations. The constant $\lambda \in \mathrm{R}^+$ is a scalar that determines the diffusion rate, and $\eta_s$ represents the spatial neighborhood of pixel $s$. Perona and Malik linearly approximated the gradient using nearest-neighbor differences in a particular direction as

$$\nabla u_{s,p} = u_p - u_s. \tag{4}$$

## 3 AFMPDE-based Small Target Detection Algorithm

Although target detection algorithms have steadily improved, many of them still failed to work robustly during applications that involve changing backgrounds that are frequently encountered. In general, a small target embedded in a cloudy background appears as a gray spot in an image, which also contains bright illuminated terrain or sunlit clouds. In this case, clutter is often more intense than both the sensor noise and the target signal, and therefore the adaptive filters as isotropic filters, such as local mean removal (LMR), TDLMS, or the differencing operation are insufficient to discriminate the target from the bright clutter.

In this paper we present a novel AFMPDE algorithm to overcome these shortcomings. Three significant improvements are made: (1) different the conditions on weighting function $c(t)$ is presented for clutter removal and target-enhancement regularization; (2) the conventional two sequential processing steps (background estimation and target enhancement) of the clutter removal procedure are merged into one step in which the tasks of the clutter removal and target enhancement are achieved simultaneously; and (3) the computational complexity of the iterations in Eq. (3) and conventional multistep processing are reduced to obtain much faster performance.

### 3.1 *Conditions of Clutter Removal and Target-Enhancement Regularization*

Since the clutter-removal procedure is used to reduce the effects of nonstationary background on detection performance, it must satisfy two basic requirements: (1) it must remove the background structures in the image to reduce the number of false alarms in the detection step, and (2) it must maintain a high SCR to avoid detection probability reduction. Therefore, to encourage smoothing within a region and across boundaries and to discourage smoothing in the signal of interest, we propose the following modified conditions on the weighting function $c(t) = \varphi'(t)/2t$.

Basic conditions: $\varphi'(t) \geq 0, \forall t \geq 0; \varphi(t) \geq 0, \forall t$ with $\varphi(0) = 0$; $\varphi(t) = \varphi(-t)$;
$\varphi(t)$
continuously differentiable.

New conditions for clutter removal and target enhancement:

i. $\varphi'(t)/2t$
continuous and strictly monotonous increasing on $[0, +\infty)$ to avoid instabilities; (5.1)

ii. $\lim_{t \to +\infty} \varphi'(t)/2t = M, M \in [0, +\infty)$:

using anisotropic diffusion of edges to reduce structured background clutter; (5.2)

iii. $\lim_{t \to +0} \varphi'(t)/2t = 0$:

isotropic smoothing in homogeneous areas to remove background. (5.3)

**Table 1** New weighting functions with clutter removal and target-enhancement regularization.

| No. | New weighting function $\phi(t)$ with regularization | Edge-preserving function: Function | Ref. |
|---|---|---|---|
| 1 | $1-1/[1+(t/k)^2]$ | $1/(1+t^2)$ | 10 |
| 2 | $1-\exp[-(t/k)^2]$ | $\exp[-t^2]$ | 10 |
| 3 | $1-\tanh(t)/2t$ | $\tanh(t)/2t$ | 15 |
| 4 | $1-1/\sqrt{1+(t/k)^2}$ | $1/\sqrt{1+(t/k)^2}$ | 16 |

The basic conditions define the basic restrictions, while conditions (i) to (iii) are the restrictions for clutter removal and target enhancement. They are quite different from the conditions of the edge-stopping applications in Refs. 10 to 13. These old applications recommended a monotonic decreasing function; on the contrary, we recommend a monotonic increasing function. The characteristic of the new principle is investigated in Sec. 3.2.

## 3.2 *AFMPDE Filter Formulation*

According to the new principle in Sec. 3.1, we first start with the Geman-Meclure regularization[14] to analyze the smoothing effect of the regularization functional $J$ on the pixel $u(i,j)$. The regularization term $J$ is formulated as

$$J(u)=\int \varphi(u_x,u_y)dxdy. \tag{6}$$

It is discretized in four-nearest neighbors $D_u$ as

$$J(u)=\sum_{i,j\in D_u}\{\varphi[D^x_{i,j}(u)]+\varphi[D^y_{i,j}(u)]\}, \tag{7}$$

where $D^x_{i,j}(u)=(u_{i,j+1}-u_{i,j})$, $D^y_{i,j}(u)=(u_{i+1,j}-u_{i,j})$. The effect of the change of pixel $u(i,j)$ on $\partial J/\partial u_{i,j}$ is formulated as

$$\begin{aligned}\frac{\partial J}{\partial u_{i,j}}&=\frac{\partial}{\partial u_{i,j}}[\varphi(u_{i,j+1}-u_{i,j})+\varphi(u_{i,j}-u_{i,j-1})+\varphi(u_{i+1,j}-u_{i,j})\\&\quad+\varphi(u_{i,j}-u_{i-1,j})]=-\varphi'(u_{i,j+1}-u_{i,j})\\&\quad+\varphi'(u_{i,j}-u_{i,j-1})-\varphi'(u_{i+1,j})-\varphi'(u_{i+1,j}-u_{i,j})\\&\quad+\varphi'(u_{i,j}-u_{i-1,j}).\end{aligned} \tag{8}$$

Using $\varphi'(t)=2t[\varphi'(t)/2t]=2t\times c(t)$, Eq. (8) can be rewritten as

$$\frac{\partial J}{\partial u_{i,j}}=-2\{\lambda_E u_{i,j+1}+\lambda_W u_{i,j-1}+\lambda_N u_{i+1,j}+\lambda_S u_{i-1,j}-\lambda_\Sigma u_{i,j}\}, \tag{9}$$

and

$$\lambda_E=c(u_{i,j+1}-u_{i,j}),\quad \lambda_W=c(u_{i,j-1}-u_{i,j}),$$
$$\lambda_N=c(u_{i+1,j}-u_{i,j}),\quad \lambda_S=c(u_{i-1,j}-u_{i,j})$$

$$\lambda_\Sigma=\lambda_E+\lambda_W+\lambda_N+\lambda_S. \tag{10}$$

In other words, the derivative of $J$ at the pixel $(i,j)$ is obtained by convolving the original image $u$ with the kernel $C'_w$. That is,

$$\hat{u}=C'_w*u,\quad\text{and}\quad C'_w=\begin{bmatrix}0&-\lambda_N&0\\-\lambda_W&\lambda_\Sigma&-\lambda_E\\0&-\lambda_S&0\end{bmatrix}, \tag{11}$$

where $\hat{u}$ is the filtered image. Therefore, $C'_w$ is a local adaptive weighted Laplacian filter whose weights are given by the weighting function $c(t)$. By recording the new $c(t)$ as $\phi(t)$ according to Eq. (5), then the functions $\phi(t)$ in Table 1 are feasible for small-target detection in IR clutter.

## 3.3 *Characteristics of AFMPDE Filter Responding to Different Signal*

The first case is that of a homogeneous area of the image: All gradients around the pixel $(i,j)$ are close to zero. Because $\phi(t)=\varphi'(t)/2t$ meets condition (iii) in Sec. 3.1, all weights around the pixel $u_{i,j}$ are approximately zero. The operator $C'_w(\varepsilon)$ is shown in Table 2 (column A), where $\lim_{\varepsilon\to 0}C'_w(\varepsilon)=0$. Thus, $u_{i,j}$ is completely smoothed (removed) as stationary clutter background.

Another case is that of similar large gradients around $u_{i,j}$: All gradients are equal to $t=|\nabla|\gg 0$. According to condition (ii), $\lim_{t\gg 0}\phi(t)=m$, and $C'_w(m)$ is given in Table 2 (column B). Then Eq. (9) is expressed as

**Table 2** Filtering kernel $C'_w$ around pixel $(i,j)$ in different conditions.

| A | B | C |
|---|---|---|
| $C'_w(\varepsilon)=\begin{bmatrix}0&-\varepsilon&0\\-\varepsilon&4\varepsilon&-\varepsilon\\0&-\varepsilon&0\end{bmatrix}$ In a homogeneous area | $C'_w(m)=\begin{bmatrix}0&-m&0\\-m&4m&-m\\0&-m&0\end{bmatrix}$ In a similar large-gradient (target-related) area | $C'_w(e)=\begin{bmatrix}0&-e&0\\0&2e&0\\0&-e&0\end{bmatrix}$ In an edge or boundary structured area |

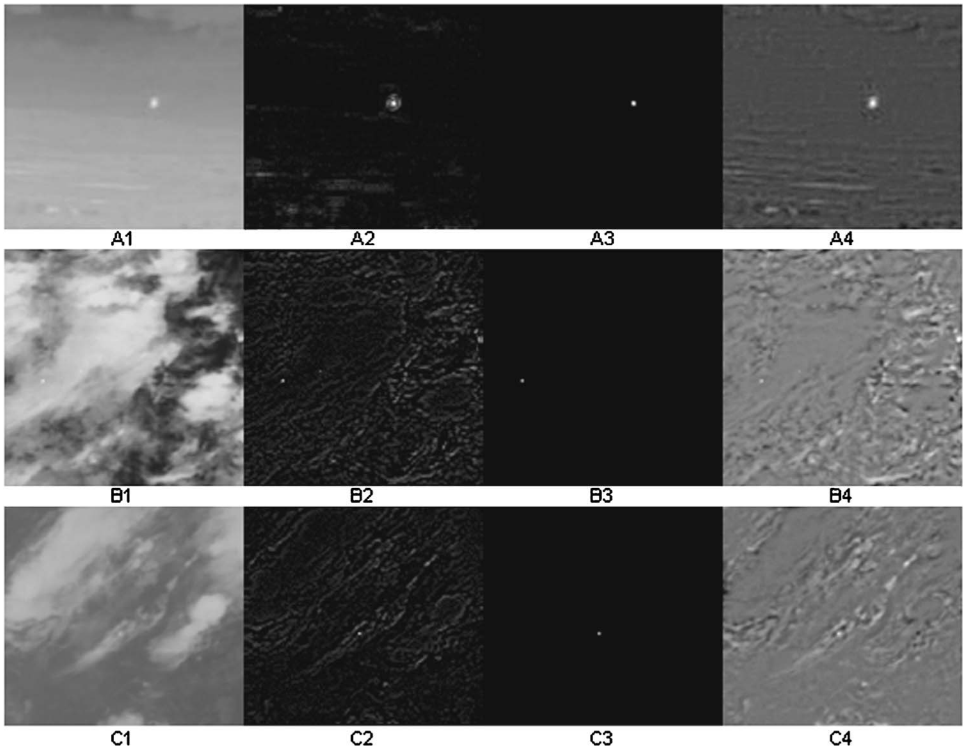


**Fig. 1** Original image and resulting images. A1, B1, C1: original IR images in different backgrounds. A2, B2, C2: AFMPDE's filtered results of A1, B1, C1. A3, B3, C3: thresholding of A2, B2, C2, respectively. A4, B4, C4: TDLMS's filtered results of A1, B1, C1.

$$\frac{\partial J}{\partial u_{i,j}} = 4\phi(t) \times t \quad \propto t, \tag{12}$$

where $\propto$ is a direct proportional sign and Eq. (12) increases as $t$ increases because of condition (i); that is, a filtered signal with a great gradient will be enhanced. It is known that a small-target signal can be modeled as a 2-D pulse of small spatial extent, which is well approximated by the sensor point spread function (PSF) and occupies only a few adjacent columns in an IR image.[1,17,18] Given such condition, $u_{i,j}$ with similar high variations (assuming they are generated by small targets) will be enhanced prominently by $C'_w(m)$.

The last case is an edge or boundary. For example, there is a line edge passing through $u_{i,j}$. The corresponding $C'_w(e)$ is shown in Table 2 (column C). Thus, $u_{i,j}$ with variations (assuming they are due to edges) will not be enhanced as much as in the case of Table 2 (column B); in other words, the structured clutter is smoothed more than in the previous case.

The analyses show that $C'_w$ is a local adaptive anisotropic filter. In contrast with conventional filters (LMR, TDLMS), an AFMPDE filter's role is twofold: In the stationary area with a small gradient, $C'_w$ is an isotropic diffusion filter to eliminate stationary clutter background; in the nonstationary area with a great gradient, $C'_w$ becomes an anisotropic diffusion filter to smooth the background structure more, and at the same time maintain the signal of interest as sharp and stable. In short, its role is to enhance the signal of interest while reducing complicated textured clutter, both locally and adaptively. Such *a priori* constraints on filtering preprocessing are called clutter removal and target-enhancement regularization.

### 3.4 *AFMPDE-based Small-Target Detection Algorithm*

To detect small targets in IR images using an AFMPDE filter, first we use Eqs. (10) and (11) to process the original image $u$ by convolving with $C'_w$, and then use a proper threshold to separate the target signal from the filtered image $\hat{u}$. The processing determines candidates for targets in every frame of the images. Then we could use a multiframe accumulation method, autocorrelation, a time-predicting algorithm, velocity filtering theory, etc., to suppress the random noise. After the cluttered background and random noise suppression, we can use dynamic programming, pipeline filtering, the Hough transform, a trajectory matching algorithm, etc., to estimate the target trajectories.

## 4 Experimental Results

### 4.1 *Performance Criteria*

Two criteria are defined to measure the capability of different filters to preserve the target signal and remove the background structures, respectively; the computational complexity (elapsed time, EST) is also used.

The capability of target preservation is measured using the improvement in SCR (ISCR) comparison of the SCR obtained after clutter removal ($SCR_{\mathrm{out}}$) with the original SCR ($SCR_{\mathrm{in}}$) in the original image. The ability to remove

**Table 3** Performance comparison of different methods in different clutter.

| Images | | | TDLMS | | | AFMPDE | | |
|---|---|---|---|---|---|---|---|---|
| Frame no. | Target size | $SCR_{in}$ | ISCR | BSF | EST(s) | ISCR | BSF | EST(s) |
| A1 | 6×6 | 2.397 | 7.172 | 1.430 | 0.040 | **10.108** | **3.208** | **0.010** |
| B1 | 3×3 | 0.985 | 1.414 | 3.084 | 0.045 | **1.990** | **4.074** | **0.010** |
| C1 | 1×1 | 1.560 | 6.900 | 2.402 | 0.040 | **17.18** | **3.768** | **0.010** |

the background structures is measured by the background suppression factor (BSF). They are defined as

$$\mathrm{SCR} = \frac{|\mu_{bt} - \mu_b|}{\sigma_c}, \tag{13}$$

$$\mathrm{ISCR} = \frac{SCR_{\mathrm{out}}}{SCR_{\mathrm{in}}}, \tag{14}$$

and

$$\mathrm{BSF} = \sigma_{\mathrm{in}}/\sigma_{\mathrm{out}}, \tag{15}$$

where $\mu_{bt}$ is the intensity peak value of the target, $\mu_b$ is the average intensity value of the pixels in the neighbor area around the target, and $\sigma_c$ is the background plus noise standard variance. $\sigma_{\mathrm{in}}$ and $\sigma_{\mathrm{out}}$ are background standard deviations of the original image and the filtered image, respectively.

### 4.2 *Experiments Using Real IR Images*

We estimate the performance of the AFMPDE method by comparisons with TDLMS. For these experiments, we select typical IR images from different image sequences. Figure 1 shows the filtered effect of several real IR images with different clutter backgrounds. The $\phi(t)$ function used is the second function in Table 1, $\phi(t) = 1 - \exp(-t^2)$, and the experimental results are listed in Table 3. It is obvious that AFMPDE maintains better performance for small-target detection under different backgrounds and diverse target sizes (1×1 to 6×6 pixels), especially in seriously cluttered backgrounds such as Fig. 1 (B1, C1). AFMPDE suppresses the background structures much better than TDLMS. Table 3 also shows that AFMPDE takes much less computational time.

### 4.3 *Experiments Using Image Sequences*

To further evaluate the performance, AFMPDE is tested in a sequence of IR images. The sequence contains 28 frames, the targets' size is about 3×3 pixels, and the speed of the target is about 2 to 4 pixels per frame. The weighting function is also the second function in Table 1, and the segmentation threshold equals 160. Figure 2 depicts the performance comparison of TDLMS and AFMPDE. Figure 3 gives the value of ISCR and BSF of every frame image of the sequence filtered by the algorithms, respectively. Figure 2 shows that filtered results of TDLMS still include many high, light-clutter patches and textured edges, and the remaining structured clutter leads to degraded detectability and a high false-alarm rate in sequential target detection and tracking. In contrast with TDLMS, AFMPDE does well in these aspects. This shows that AFMPDE preserves the small-target signal and at the same time removes the background structures much better than TDLMS.

## 5 Conclusion

Anisotropic diffusion technologies based on the PDE model are usually used in many conventional applications. In this paper, by analyzing the signal characteristic of the target, background, and noise, we modified the weighting functions and presented a novel adaptive anisotropic filter

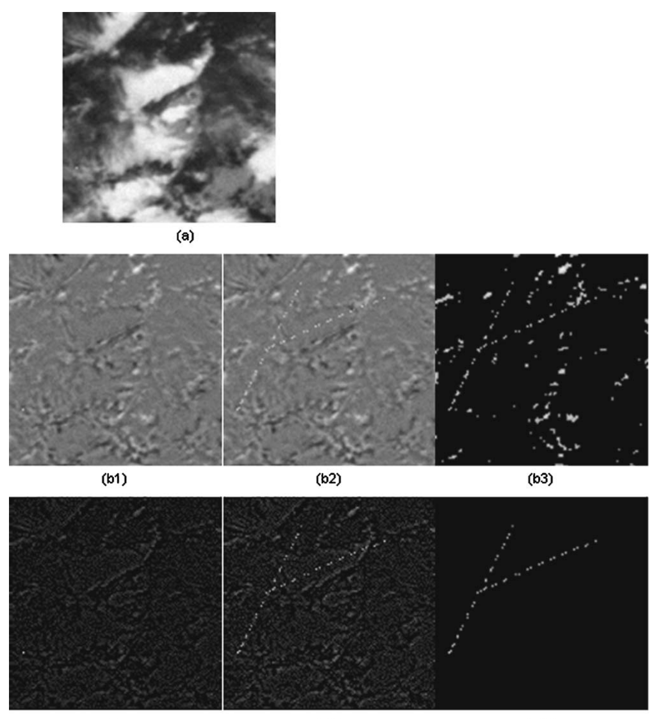


**Fig. 2** Performance comparison of TDLMS and the proposed AFMPDE. (a) The first frame of the image sequence. (b1) The first frame of the TDLMS's filtered results. (b2) The projection of all the TDLMS's filtered results on a time coordinate. (b3) Segmented result of (b2). (c1) The first frame of the AFMPDE's filtered results. (c2) The projection of all the AFMPDE's filtered results on a time coordinate. (c3) Segmented result of (c2).

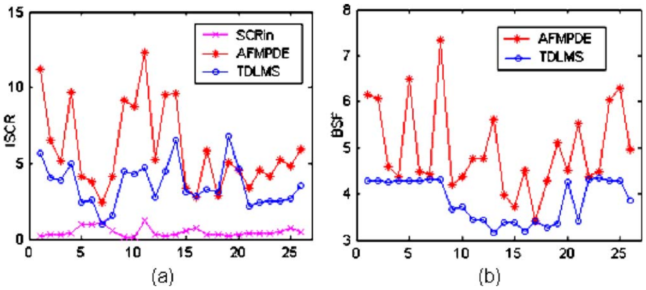


**Fig. 3** Experimental comparative analysis of image sequence. (a) ISCR with respect to frame number of image sequence; (b) BSF values with respect to frame no. of image sequence.

applied to a new problem of small-target detection in IR cluttered images. We converted the new weighting functions into an operator with clutter-removal and target-enhancement regularization. We also gave a heuristic study of new conditions on the weighting function for such a regularizing operator. Therefore, such a filter's role is twofold: the signal of interest is enhanced, while complicated structured clutter is adaptively removed locally. We illustrated the performance comparisons of the proposed method and the existing method applied to IR images under real-world conditions. The experimental results demonstrate that our method can improve dim small-target detectability in a strong, structured, cluttered background and provide a robust and real-time performance.

## Acknowledgment

The work was supported by National Natural Science Foundation of China (No. 60135020).

## References


1. Steven D. Blostein and Haydn S. Richardson, "A sequential detection approach to target tracking," *IEEE Trans. Aerosp. Electron. Syst.* **30**(1), 197–212 (1994).
2. H. E. Rauch, W. I. Futterman, and D. B. Kemmer, "Background suppression and tracking with a staring mosaic sensor," *Opt. Eng.* **20**(1), 103–110 (1981).
3. D. S. K. Chan, D. A. Langan, and D. A. Stayer, "Spatial processing techniques for the detection of small targets in IR clutter," *Proc. SPIE* **1305**, 53–62 (1990).
4. B. Porat and B. Friedlander, "A frequency domain algorithm to multiframe detection and estimation of dim targets," *IEEE Trans. Pattern Anal. Mach. Intell.* **12**(4), 398–401 (1990).
5. J. N. Lin, X. Nie, and R. Unbehauen, "Two-dimensional LMS adaptive filter incorporating a local-mean estimator for image processing," *IEEE Trans. Circuits Syst., II: Analog Digital Signal Process.* **40**(7), 417–428 (1993).
6. Meng Li, Tianxu Zhang, et al., "Moving weak point target detection and estimation with three-dimensional double directional filter in IR cluttered background," *Opt. Eng.* **44**(10), 1070071-4 (2005).
7. D. Wang, "Adaptive spatial/temporal/spectral filters for background clutter suppression and target detection," *Opt. Eng.* **21**, 1033–1038 (1982).
8. K. A. Melendez and J. W. Modestino, "Spatio-temporal multiscan adaptive matched filtering," *Proc. SPIE* **2561**, 51–65 (1995).
9. D. M. Silva, et al., "Optimal detection of small targets in a cluttered background," *Opt. Eng.* **37**(1), 83–92 (1998).
10. P. Perona and J. Malik, "Scale-space and edge detection using anisotropic diffusion," *IEEE Trans. Pattern Anal. Mach. Intell.* **12**(7), 629–639 (1990).
11. S. Teboul, B. C. Laure, et al., "Variational approach for edge-preserving regularization using coupled PDE's," *IEEE Trans. Image Process.* **7**(3), 387–397 (1998).
12. S. C. Park and M. G. Kang, "Noise-adaptive edge-preserving image restoration algorithm," *Opt. Eng.* **39**(12), 3124–3137 (2000).
13. Y.-C. Song and D.-H. Choi, "Scale-based image enhancement using modified anisotropic diffusion filter," *Opt. Eng.* **43**(9), 2094–2099 (2004).
14. S. Geman and D. E. McClure, "Bayesian image analysis: An application to single photon emission tomography," in *Proc. Stat. Comput. Sec., American Statistical Association*, Washington, DC, 12–18 (1985).
15. P.-J. Green, "Bayesian reconstruction from emission tomography data using a modified EM algorithm," *IEEE Trans. Med. Imaging* **9**, 84–93 (1990).
16. P. Charbonnier, L. Blanc-F'eraud, et al., "Deterministic edge-preserving regularization in computed imaging," *IEEE Trans. Image Process.* **6**(2), 298–311 (1997).
17. D. H. Xue, "An extended track-before detect algorithm for infrared target detection," *IEEE Trans. Aerosp. Electron. Syst.* **33**(3), 1087–1092 (1997).
18. D. S. K. Chan, D. A. Langan, and D. A. Staver, "Spatial processing techniques for the detection of small targets in IR clutter," *Proc. SPIE* **1305**, 53–62 (1990).


**Biyin Zhang** graduated from China University of Geosciences, China, in 2001. Since September 2001, he has studied for his MS and PhD degrees in pattern recognition and intelligence systems from Huazhong University of Science and Technology. He is currently a PhD candidate at Huazhong University of Science and Technology. His research interests include image processing, computer vision, target recognition, and performance evaluation.

**Tianxu Zhang** graduated from the University of Science and Technology of China. He received his MS degree in computer science from Huazhong University of Science and Technology, China, in 1983, and his PhD degree in biomedical engineering from Zhejiang University, China, in 1989. He is currently a professor and director of the Institute for Pattern Recognition and Artificial Intelligence, Huazhong University of Science and Technology, China. His research interests include image processing, computer vision, pattern recognition, and medical imaging.

**Zhiguo Cao** received his BS degree in electrical engineering from the University of Electronic Science and Technology of China in 1985, then received his MS degree in communication and information system and his PhD degree in pattern recognition and intelligence systems from Huazhong University of Science and Technology in 1990 and 2001, respectively. He is currently a professor and associate director of the Institute for Pattern Recognition and Artificial Intelligence, Huazhong University of Science and Technology, China. His research interests include image analysis, target recognition, and computer vision.

**Kun Zhang**: Biography and photograph not available.